Materials and Design 76 (2015) 230–243

Contents lists available at ScienceDirect

Materials and Design

journal homepage: www.elsevier.com/locate/matdes

Numerical – Experimental correlation of microstructures, cooling rates and mechanical properties of AISI 1045 steel during the Jominy end-quench test

César R.N. Nunura [a,*], Carlos A. dos Santos [a], Jaime A. Spim [b]

[a] Metallic Materials Research Group, School of Engineering, Pontifícia Universidade Católica do Rio Grande do Sul, Porto Alegre, RS, Brazil
[b] Foundry Laboratory, School of Engineering, Universidade Federal do Rio Grande do Sul, Porto Alegre, RS, Brazil

ARTICLE INFO

Article history:
Received 21 February 2014
Revised 13 March 2015
Accepted 19 March 2015
Available online 20 March 2015

Keywords:
Jominy end-quench test
AISI 1045 steel
Cooling rate
Austenitizing temperature
Microstructure
Hardness

ABSTRACT

This work addresses the numerical correlation of the factors that may affect the hardenability of AISI 1045 steel submitted to the Jominy end-quench test in three austenitizing temperatures: 20 °C, 70 °C and 120 °C above the critical temperature (A_{c3}) according to the CCT diagram (Continuous Cooling Transformation). Thermocouples were placed in the specimens at predefined points to obtain cooling curves during the Jominy end-quench test. Metallographic analysis and the Jominy hardness profiles (using the Rockwell C method) allowed evaluating the hardenability in function of the austenitizing temperatures. Calculation of the percentage of phases presented in the microstructures and Vickers microhardness tests at these phases and micro-constituents were applied to obtain numerical expressions to correlate the phase percentages and hardness profiles according to the cooling rate variations during the test. Subsequently, equations were obtained by regression numerical methods to estimate the amount of phases and micro-constituents (martensite, bainite, pearlite and ferrite) formed during the test, and also to estimate the hardness profile.

1. Introduction

The Jominy end-quench test which follows ASTM: A-255, is used to measure the hardenability of steels. It consists on heating of a standardized cylindrical specimen of material in test (25.4 mm diameter and 100.0 mm in length) until the austenitizing temperature, and then cooling it at one end through of water in order to induce the formation of the martensitic structure. After that, the hardness is measured along the specimen at intervals of 1.59 mm between each measure. Obviously, the first measure presents high values of hardness due to the formation of martensite by high cooling water. Consequently, the hardness decreases in more distant positions of the cooled surface, because in these points, the cooling rates are lower resulting in the formation of phases such as ferrite, pearlite and bainite.

Some publications have shown interest in understand the phenomena of heat transfer and phase transformation of austenite during cooling. Homberg [1] has presented a numerical algorithm for simulating the Jominy end-quench test and deriving continuous cooling diagrams for AISI 1080 steel. The underlying mathematical model for the austenite–pearlite phase transition is based on Scheil's Additivity Rule and the Johnson–Mehl equation. Le Masson et al. [2] have developed a numerical method for the two-dimensional estimation of the convection heat transfer coefficient for a rapid metallurgical heat treatment. Mathematical modeling of austenite decomposition has also been investigated by Smoljan [3]. Phase portion in steel was predicted based on hardenability curve of the Jominy-specimen. The designed inverse method of prediction austenite decomposition was used in computer simulation of microstructure transformation during the austenite decomposition of DIN C 45 steel. Finite element simulations that predict the microstructure and properties of heat-treated steels can be significantly improved by incorporating appropriate models for the kinetics of various austenite transformations, and it has been investigated by Lee et al. [4] and Pietrzyk et al. [5].

Numerical models are being developed for the simulation of the cooling curves, prediction the microstructural formation of the present phases and the hardness profile obtained during the test. Smoljan et al. [6] have investigated the performance and possibilities of application of the modified Jominy-test in computer simulation of high-hardenability steel quenching. Specimens have presented similar cooling curves if the cylindrical specimen has

* Corresponding author.
E-mail address: cesar.rolando@acad.pucrs.br (C.R.N. Nunura).

http://dx.doi.org/10.1016/j.matdes.2015.03.031
0261-3069/

Table 1
Chemical composition of AISI 1045 steel specimen (wt.%).

C	Si	Mn	P	S	Cu	Cr	Ni	V	Co	W	Mo
0.45	0.19	0.70	0.02	0.03	0.12	0.05	0.05	<0.001	<0.01	<0.01	<0.005

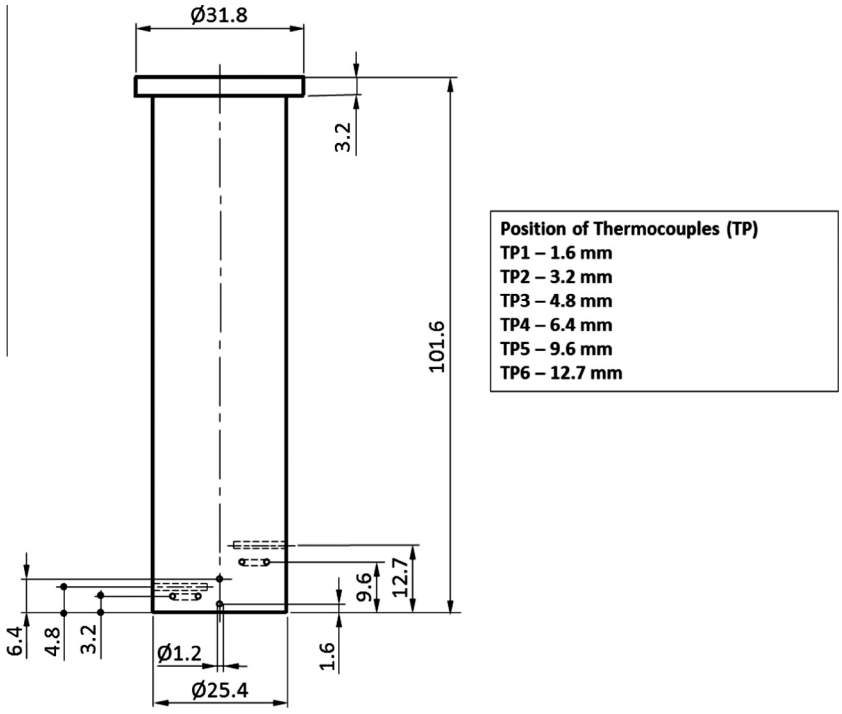

Fig. 1. Arrangement of thermocouples in Jominy specimen.

been quenched in oil or cooled in air. Zehtab et al. [7] have focused on some theories about on correlation between cooling curves and hardness of test specimen such as Quench Factor Analysis. In this research it was tried to simulate the Jominy test of a steel (AISI 4130) with the method. Song et al. [8] have proposed an improved mathematical model for simulating the Jominy end-quench curves by introducing a parameter named alloying interactions equivalent. The thermal properties, the Rockwell C hardness and the microstructure of three end-quench Jominy bar steels (C48, 42CrMo4 and 35NiCrMo16) have been investigated by Ghrib et al. [9]. The thermal properties were determined using photothermal deflection technique and the hardness was measured by Rockwell durometer. Çakir et al. [10] have investigated the hardenability of AISI 1050 steel in different cooling media using Jominy test. The temperature values were recorded using thermocouples that were placed on sample. The correlation

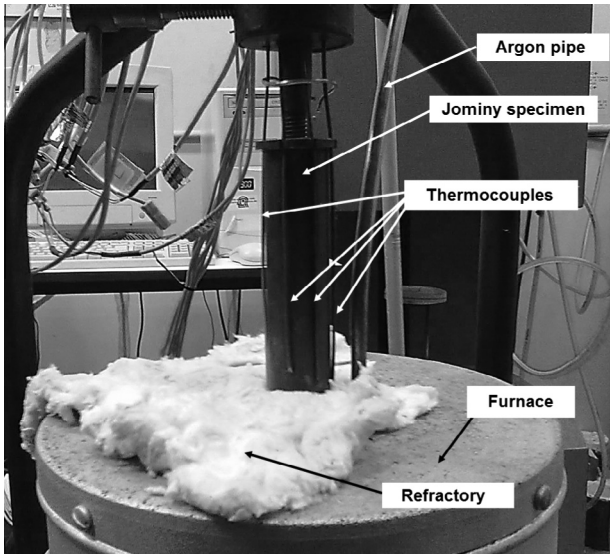

Fig. 2. Jominy specimen, thermocouples and the furnace for the test.

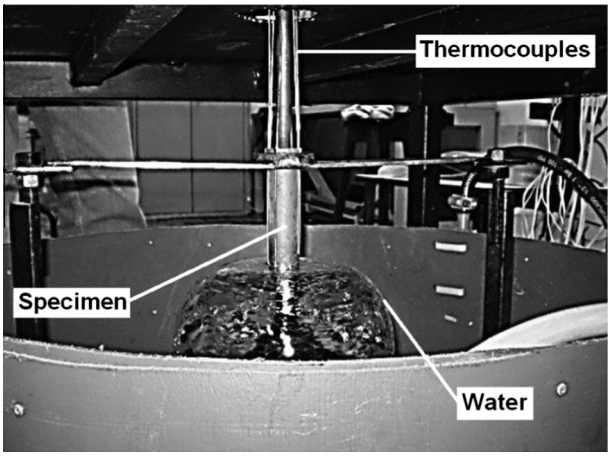

Fig. 3. Image of the cooling of the specimen.

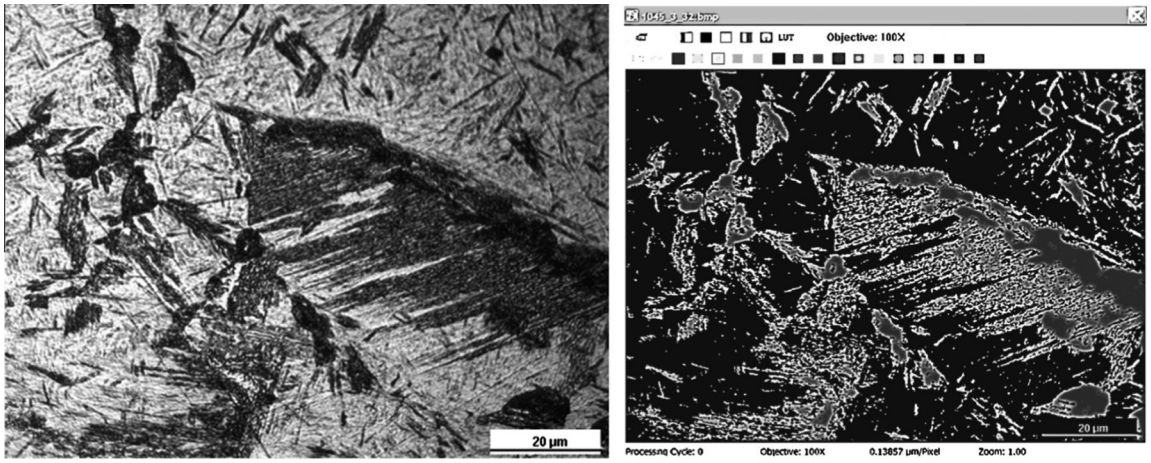

Fig. 4. Calculating the percentage of phase at the microstructure. In (a) the metallography. In (b) image processing.

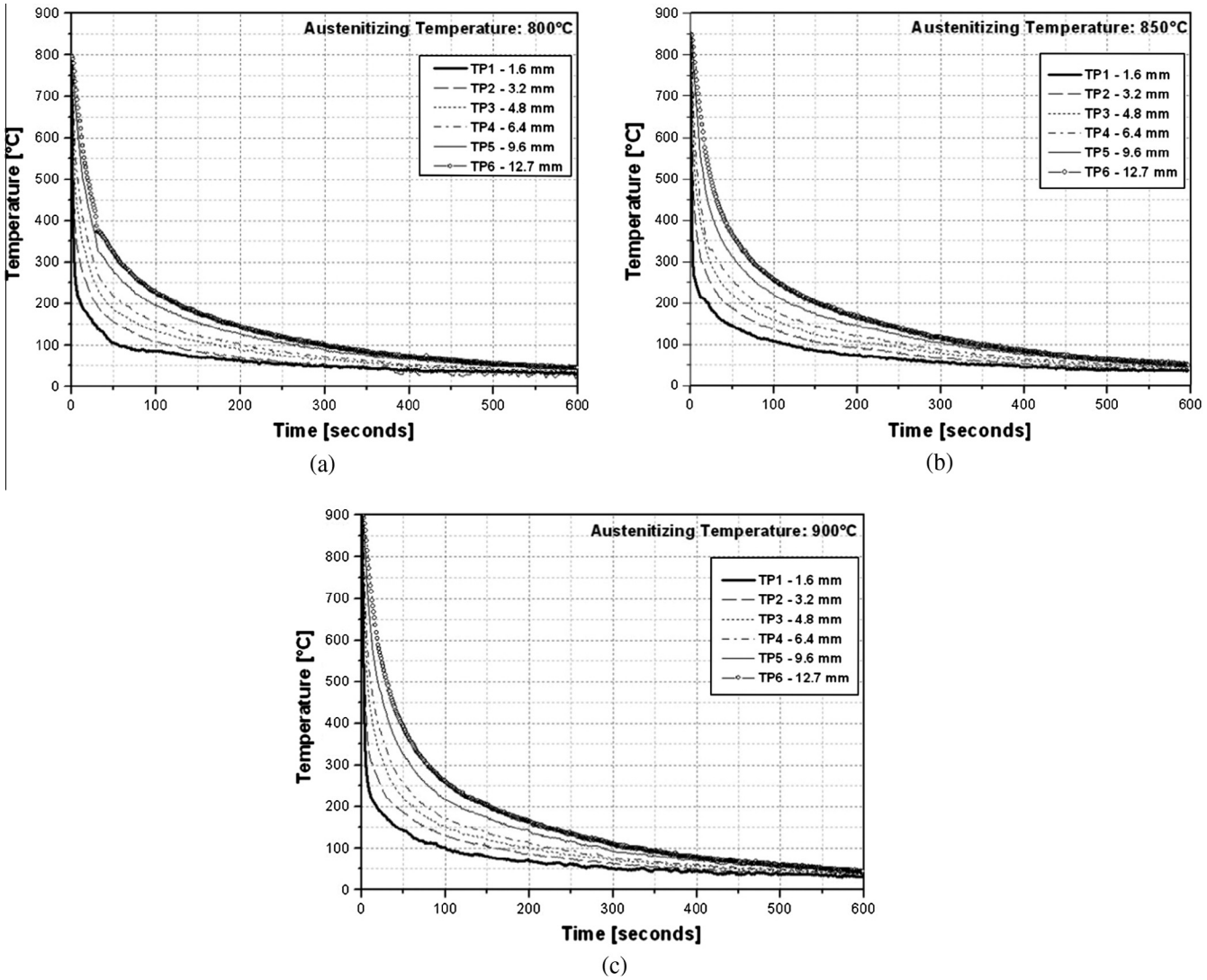

Fig. 5. Experimental cooling curves in the three austenitizing temperatures: (a) 800 °C, (b) 850 °C and (c) 900 °C.

between thermal properties and hardenability was established. When Jominy water pressure decreased, hardenability decreased in Jominy bar. But hardenability of steel quenched by air–water mixture cooling media was observed that increasing surprisingly. As a result of air–water mixture quenching, heat transfer accelerated and the hardenability increased in the Jominy bar. Finally an

Table 2
Cooling rates (°C/s) for different austenitizing temperatures.

Jominy distance (mm)	800 °C	850 °C	900 °C
1.6	238	201	158
3.2	73	56	63
4.8	25	28	24
6.4	20	23	21
9.6	13	13	12
12.7	10	9	9

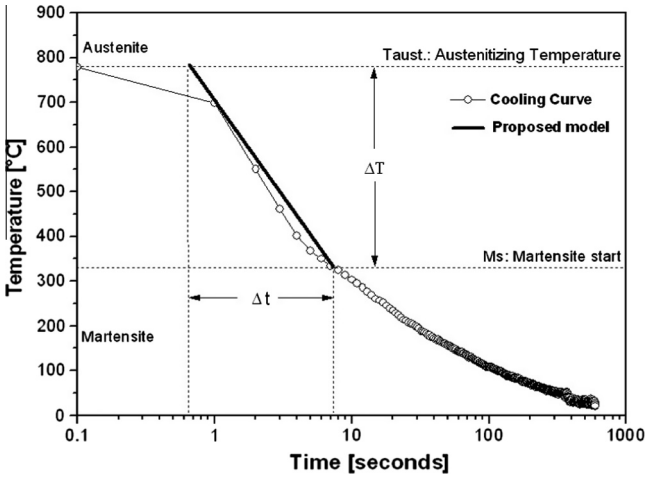

Fig. 6. Methodology for calculation of the cooling rate for austenitizing temperature of 800 °C.

Table 3
Hardness measurements (HRC) and (HV) for different temperatures austenitizing.

Distance from quenched end (mm)	800 °C		850 °C		900 °C	
	HRC	HV	HRC	HV	HRC	HV
1.6	57	633	57	633	57	633
3.2	57	633	56	613	58	653
4.8	51	528	48	484	52	544
6.4	36	354	33	327	38	372
7.9	29	294	28	286	32	318
9.6	27	279	26	272	30	302
11.1	26	272	27	279	30	302
12.7	25	253	26	272	27	279
22.2	20	238	22	248	23	254
23.8	(19)	222	20	238	23	254
25.4	(18)	219	20	238	22	248
27.0	(17)	215	20	238	21	243
28.6	(17)	215	20	238	20	238
30.2	(16)	212	(18)	219	20	238

axis-symmetric thermo-metallurgical Jominy end-quench test model was presented by Maizza et al. [11], where the heat conduction equation is coupled with an anisothermal austenite decomposition kinetic model.

The object of this work is the acquisition of the experimental cooling curves and the determination of cooling rates at specific points of the Jominy specimen, obtaining numeric expressions that permit the correlation between amount of phases and hardness as a function of the cooling rates in the specimen. Thus, it is established a correlation of cooling rates with microstructure and hardness as a function of the position. Finally, it is inserted a correlation between experimental cooling curves and Continuous Cooling Transformation diagrams (CCT).

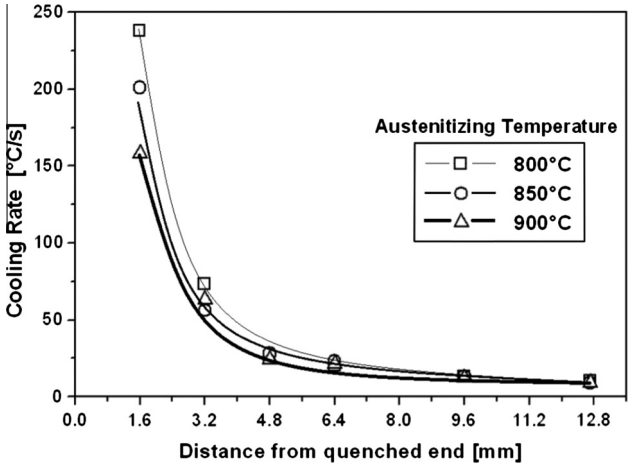

Fig. 7. Numerical adjustment of cooling rates depending on the position during the tests.

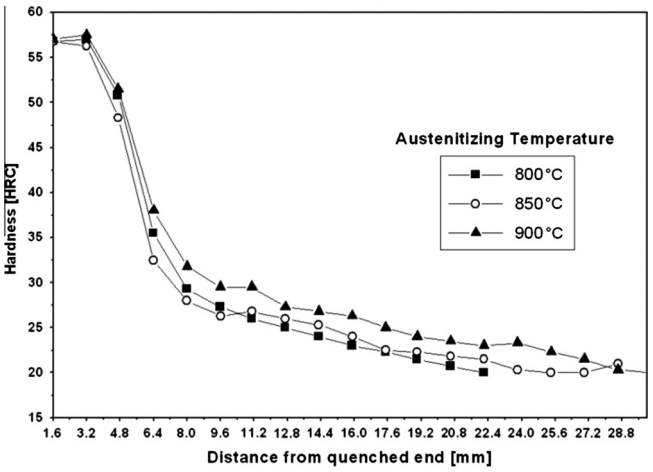

Fig. 8. Hardness profiles for different austenitizing temperatures.

2. Materials and methods

Specimens of the steel AISI 1045 were used with configuration required by ASTM: A-255. Table 1 shows the analysis by Optical Emission Spectrometry (OES) for determining the chemical composition of the steel (mass percentage).

Knowing these values, the critical temperature (A_{c3}) can be calculate and stipulate the three austenitizing temperatures for the Jominy end-quench test. Using an empirical equation from the literature [12] and the chemical composition, Eq. (1) shows the calculation of A_{c3}:

$$A_{c3} = 910 - 203\sqrt{\%C} - 15.2\%Ni + 44.7\%Si + 104\%V + 31.5\%Mo + 13.1\%W \quad (1)$$

According to austenitizing temperature, A_{c3} was determined as: 800 °C, 850 °C and 900 °C. These temperatures were determined to analyze how the austenitizing temperature can influence on the hardenability of steel.

The specimens were subjected to normalizing heat treatment before the Jominy test as required by the ASTM: A-255 standard for a period of 60 min. Within the furnace was placed a carbon-rich atmosphere to protect the specimen decarburization. During the

Jominy test, six thermocouples were placed at distances of separation of 1.6 mm from the tip cooled with the intention of obtaining cooling curves and, subsequently, calculating cooling rates. These thermocouples were placed in positions where the martensitic transformation can occur. Fig. 1 shows the arrangement of thermocouples in the specimen.

The specimens were austenitized at the temperatures for 30 min (according to ASTM: A-255). On this occasion, argon was injected into the furnace chamber (flow rate 6.0 l/min) to protect the specimen from the effects of decarburization. Concluded this interval, the specimen was removed from the oven and placed quickly in the Jominy test device. The water jet watch cools the probe tip must remain powered for 600 s. Fig. 2 shows the

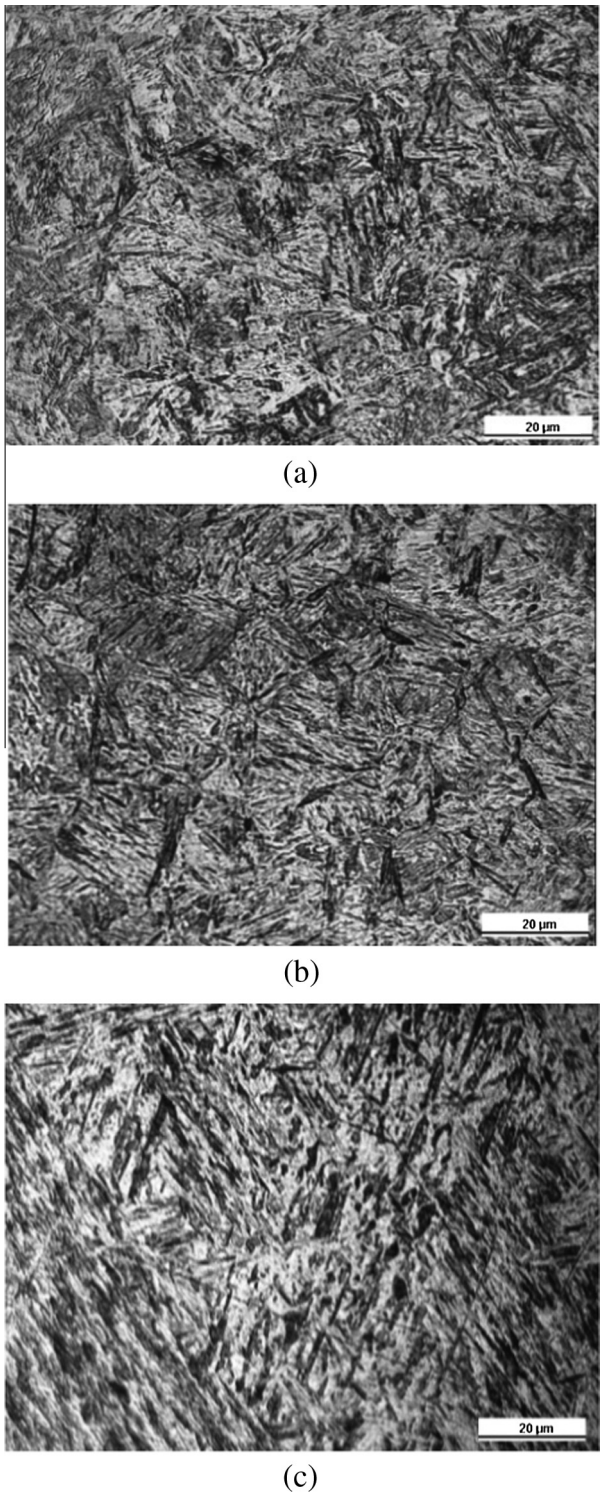

Fig. 9. Martensitic microstructures for different austenitizing temperatures. (a) 800 °C, (b) 850 °C and (c) 900 °C. Distance from quenched end: 1.6 mm. Etching: Nital 3%.

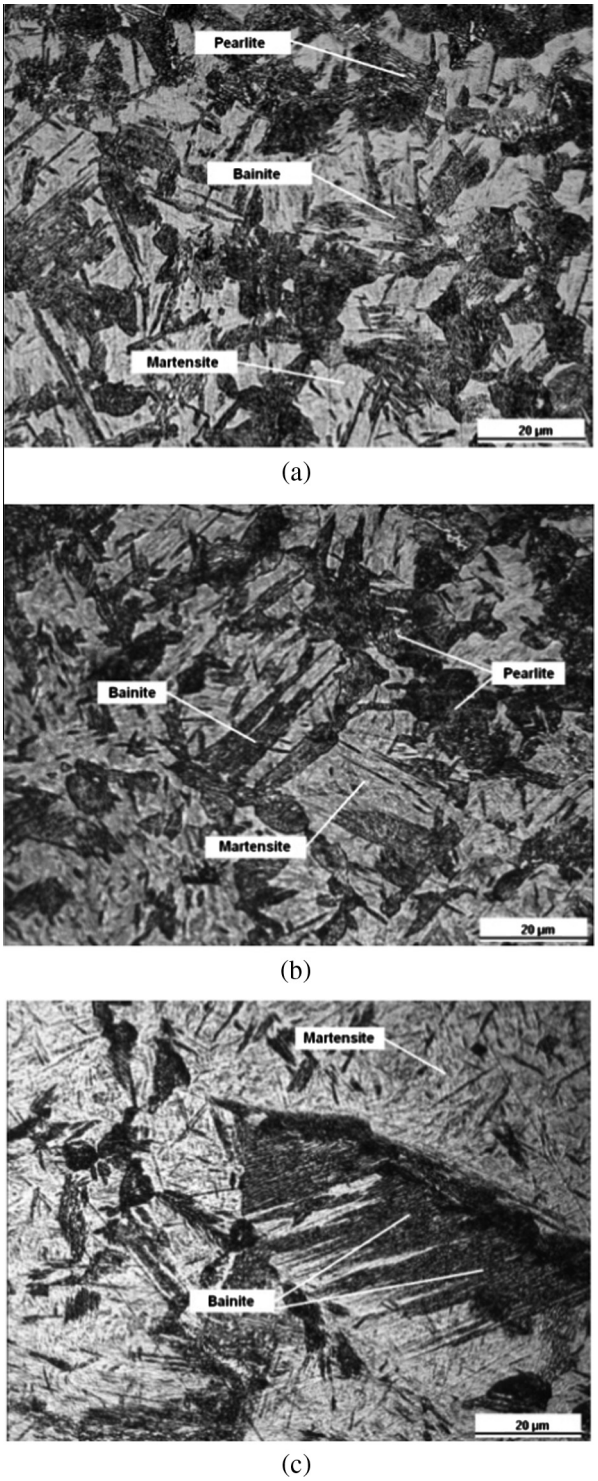

Fig. 10. Mixed microstructures after cooled during the test for different austenitizing temperatures. (a) 800 °C, (b) 850 °C and (c) 900 °C. Distance from quenched end: 4.8 mm. Etching: Nital 3%.

specimen and the furnace for the Jominy test and Fig. 3 presents a picture of the cooling of the specimen.

Using a data acquisition system it was possible to collect the monitored temperatures by thermocouples at each time during the cooling of the specimen. To calculate the cooling rates, it was used the following methodology: estimating the interval between the austenitizing temperature (T_{aust}) and the starting temperature of martensitic transformation (M_s). This (ΔT) is divided by a time interval (Δt) where the cooling rate is maximum. Eq. (2) shows the calculation of the cooling rate ($\overset{o}{T}$) in (°C/s):

$$\overset{o}{T} = \frac{\Delta T}{\Delta t} = \frac{(T_{aust} - M_s)}{\Delta t} \tag{2}$$

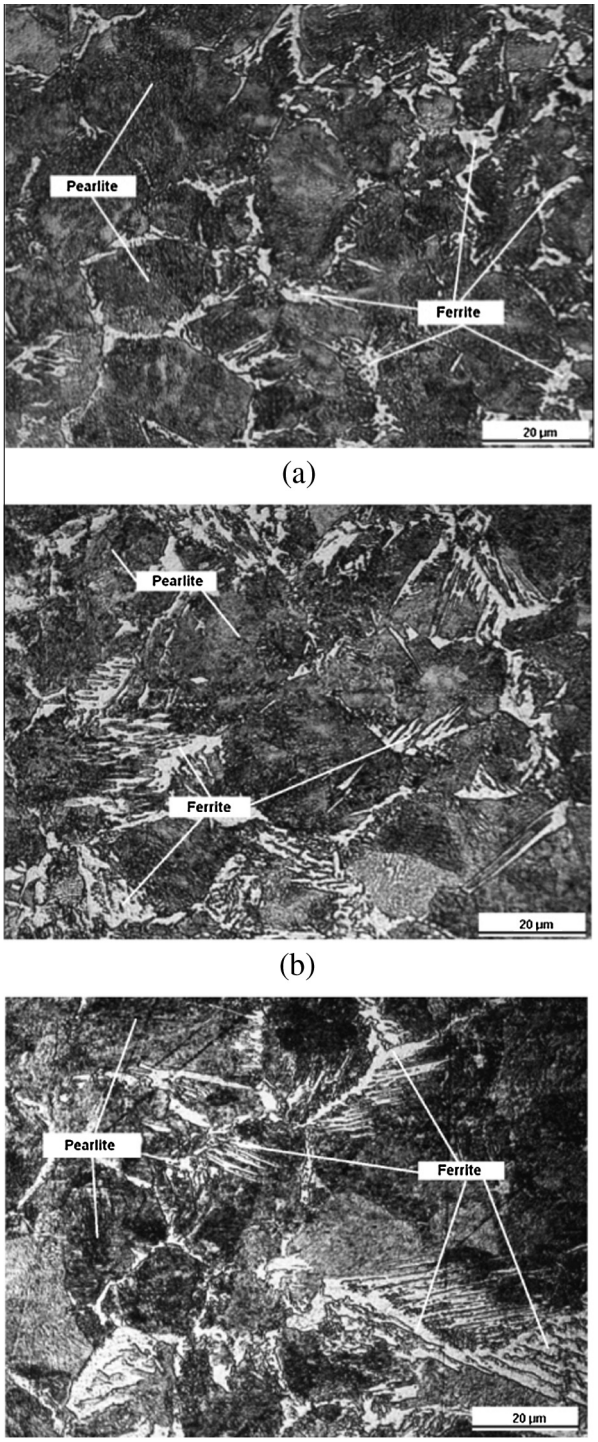

Fig. 11. Ferritic and pearlitic microstructures for different austenitizing temperatures. (a) 800 °C, (b) 850 °C and (c) 900 °C. Distance from quenched end: 12.7 mm. Etching: Nital 3%.

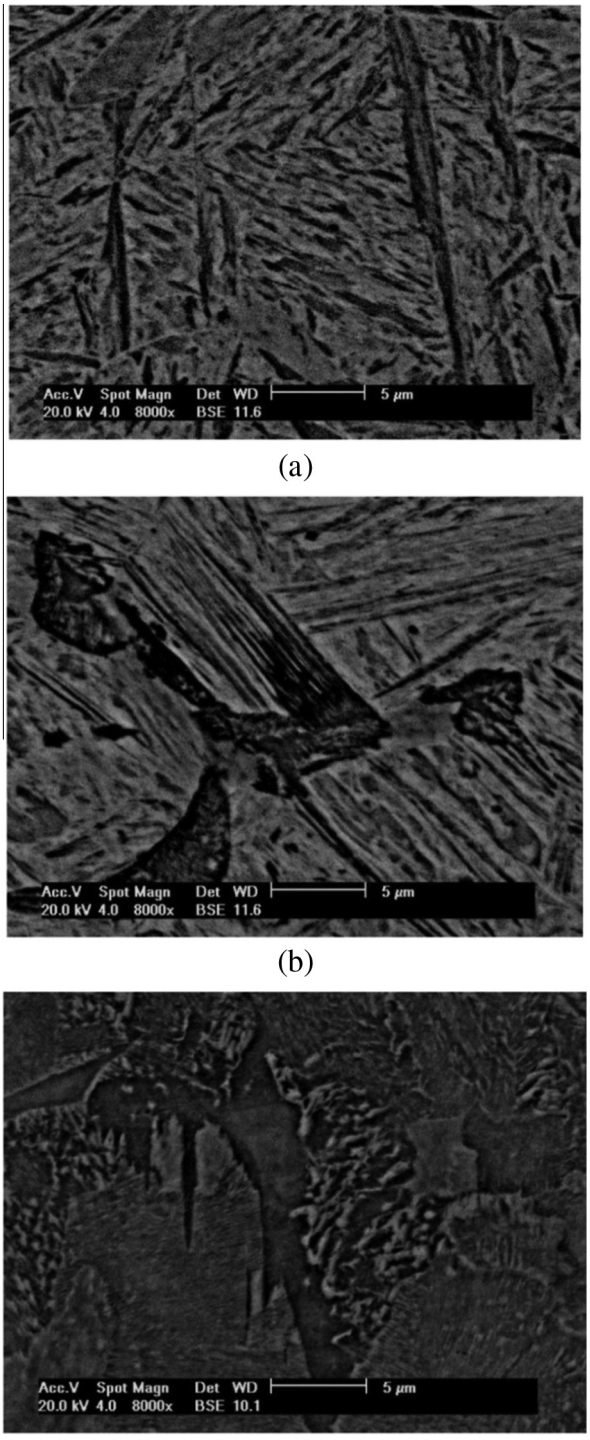

Fig. 12. Microstructures by Scanning Electronic Microscopy (SEM) as result of Jominy test for austenitizing temperature of 850 °C. In (a) martensite, (b) bainite and martensite and (c) ferrite and cementite. Etching: Nital 3%.

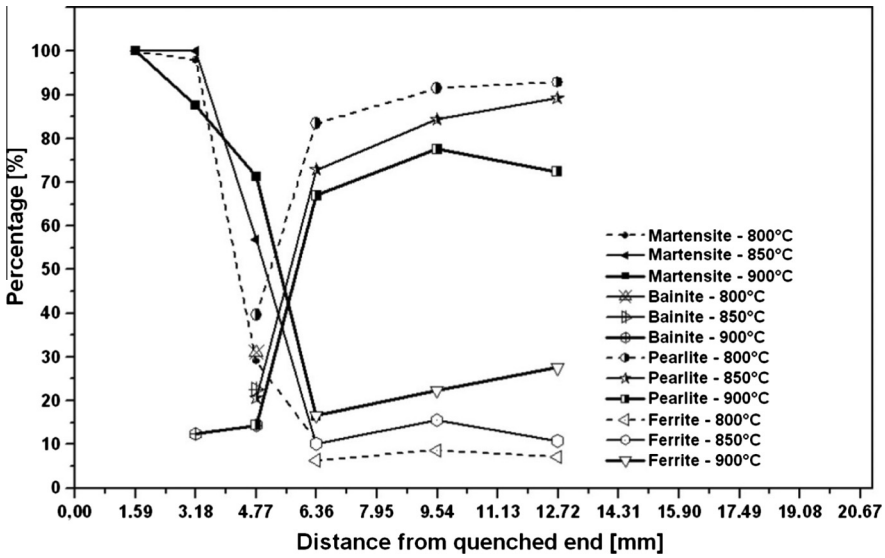

Fig. 13. Percentage of phases in function of Jominy distance for different austenitizing temperatures.

Table 4
Percentage of phases in function of Jominy distance. Austenitizing temperature: 800 °C.

Jominy distance (mm)	Martensite	Bainite	Pearlite	Ferrite	Σ%
1.6	100.0	–	–	–	100.0
3.2	98.0	2.0	–	–	100.0
4.8	29.3	31.1	39.6	–	100.0
6.4	10.3	–	83.4	6.3	100.0
9.6	–	–	91.4	8.6	100.0
12.7	–	–	92.9	7.1	100.0

Table 5
Percentage of phases in function of Jominy distance. Austenitizing temperature: 850 °C.

Jominy distance (mm)	Martensite	Bainite	Pearlite	Ferrite	Σ%
1.6	100.0	–	–	–	100.0
3.2	100.0	–	–	–	100.0
4.8	56.8	22.6	20.6	–	100.0
6.4	10.1	–	79.7	10.2	100.0
9.6	–	–	84.4	15.6	100.0
12.7	–	–	89.2	10.8	100.0

Table 6
Percentage of phases in function of Jominy distance. Austenitizing temperature: 900 °C.

Jominy distance (mm)	Martensite	Bainite	Pearlite	Ferrite	Σ%
1.6	100	–	–	–	100.0
3.2	87.6	12.4	–	–	100.0
4.8	71.2	14.4	14.4	–	100.0
6.4	16.4	–	67.0	16.6	100.0
9.6	–	–	77.6	22.4	100.0
12.7	–	–	72.4	27.6	100.0

Using an empirical equation from the literature [12], and the chemical composition of steel, Eq. (3) shows the calculation of the martensite start (M_s):

$$M_s = 512 - 453\%C - 16.9\%Ni + 15\%Cr - 9.5\%Mo + 217(\%C)^2 - 71.5\%C\%Mn - 67.6\%C\%Cr \quad (3)$$

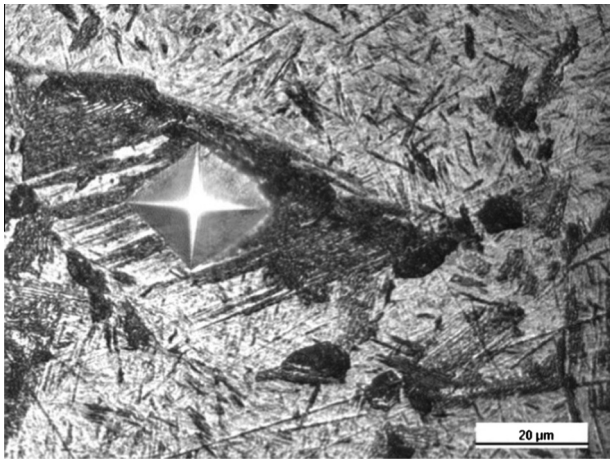

Fig. 14. Micro-indentation Vickers in a bainitic region.

Therefore, the calculated temperatures (A_{c3}) and (M_s) were: 781 °C and 328 °C, respectively.

According to ASTM: A-255, hardness measurements were performed on the specimen on the HRC scale for obtaining hardness Jominy profiles. Furthermore, Vickers microhardness tests were made subsequently at present phases in the microstructure, with loads varying of 300 g, 200 g and 25 g, with an application time of 15 s.

Micrograph results were obtained to the positions where the thermocouples were placed to estimate the percentage of formed phases during cooling with the aid of metallographic software. This tool allowed to estimate the percentage of the phases present in a micrograph with the aid of routines programmed into the software and to quantify the area of metallographic mosaics based on the color and morphology. It was used Nital 3% as metallographic etching, according to ASTM: E 3-11. The sequence of this calculation is shown in Fig. 4.

Known the microhardness and the percentage of the phases and micro-constituents present, it was possible to use Eq. (4) (mixture rule) for calculating the overall of hardness Vickers (HV) at each

point of the specimen to comparison with the results of hardness Rockwell C:

$$HV = [(\%Martensite) \cdot HV(Martensite)] + [(\%Bainite) \cdot HV(Bainite)] + [(\%Pearlite) \cdot HV(Pearlite)] + [(\%Ferrite) \cdot HV(Ferrite)] \quad (4)$$

3. Results and discussion

3.1. Experimental cooling curves

Fig. 5 shows the cooling curves at the three austenitizing temperatures: 800 °C, 850 °C and 900 °C. The positions of the six thermocouples at the specimen were explained at Fig. 1. The evolution of the thermal profile consistently compares with the results obtained by Çakir et al. [10], who used thermocouples to obtain the Jominy test cooling curves. Similar profiles in other specimens were obtained by Li et al. [13] (In a AA7050 alloy), and Ben Ammar et al. [14] (In an alloy, Zircaloy4).

3.2. Experimental cooling rates

Following the methodology described before, the cooling rates were calculated for each thermocouple position, and in each austenitization temperature as shown in Table 2. Fig. 6 shows the calculation of cooling rates for the specimen which was austenitized to 800 °C. The same methodology was used to temperatures of 850 °C and 900 °C, respectively. Points were numerically adjusted from cooling rates depending on the position for the three austenitizing temperatures according to Fig. 7, and numeric expressions were obtained.

Unlike the previously proposed method, Zehtab et al. [7] calculated cooling rates mathematically deriving the thermal profile of the test, all along the test body. Li et al. [15] used the cooling rate of the specimen when the same was 700 °C. This value was inserted into empirical equations to calculate the hardness of the martensite, bainite, pearlite and ferrite produced during the test. Lee et al. [4] used the cooling rate value of 700 °C to correlate hardness with microstructure resulting during the trial. With the method proposed in our work, concerning cooling rate, we can obtain numerical expressions for the cooling rate calculated in function of the position.

For austenitizing temperature: 800 °C

$$\overset{o}{T} = 844.7 \exp\left(\frac{x}{1.21}\right) + 11.7 \quad (5)$$

For austenitizing temperature: 850 °C

$$\overset{o}{T} = 739.8 \exp\left(\frac{x}{1.14}\right) + 13.9 \quad (6)$$

For austenitizing temperature: 900 °C

$$\overset{o}{T} = 423.2 \exp\left(\frac{x}{1.51}\right) + 10.6 \quad (7)$$

where (x) is the position or distance from quenched end (mm).

3.3. HRC hardness as a function of the austenitizing temperature

Table 3 shows the measured values of Rockwell profile for the for the three austenitizing temperatures (average of four hardness measures) which is shown in Fig. 8 and the correlation with the Vickers hardness (HV). It is observed that there was an increase in the hardenability with higher austenitizing temperature, according to Fernandino et al. [16] (in a nodular cast iron at different austenitization temperatures) and Llewellyn and Hudd [17] (at the Jominy test applied in a steel alloy).

Hardness in scale HRC is placed and the values in parentheses are outside the recommended range and are given only for comparison purposes.

3.4. Metallographic analysis

Fig. 9 shows the obtained metallographic to 1.6 mm from the tip of the specimen cooled from 800 °C, 850 °C and 900 °C, respectively. In (a) and (b) it is observed lath martensite. In (c) it is observed that in high austenitizing temperature, the martensite formed at this point adopts a coarse morphology.

In Fig. 10 it is observed that as the austenitizing temperature increases, the amount of bainitic structure formation (dark areas in the form of needles) increases followed by the formation of

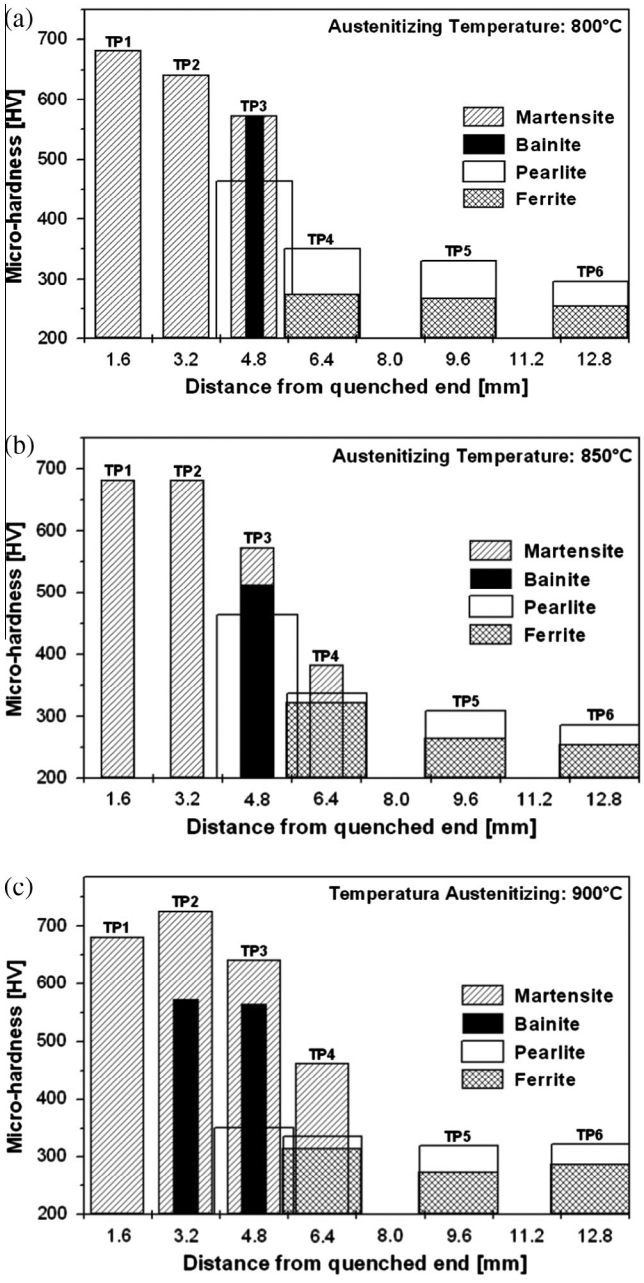

Fig. 15. Micro-hardness in function of Jominy distance for different austenitizing temperatures. (a) 800 °C, (b) 850 °C and (c) 900 °C.

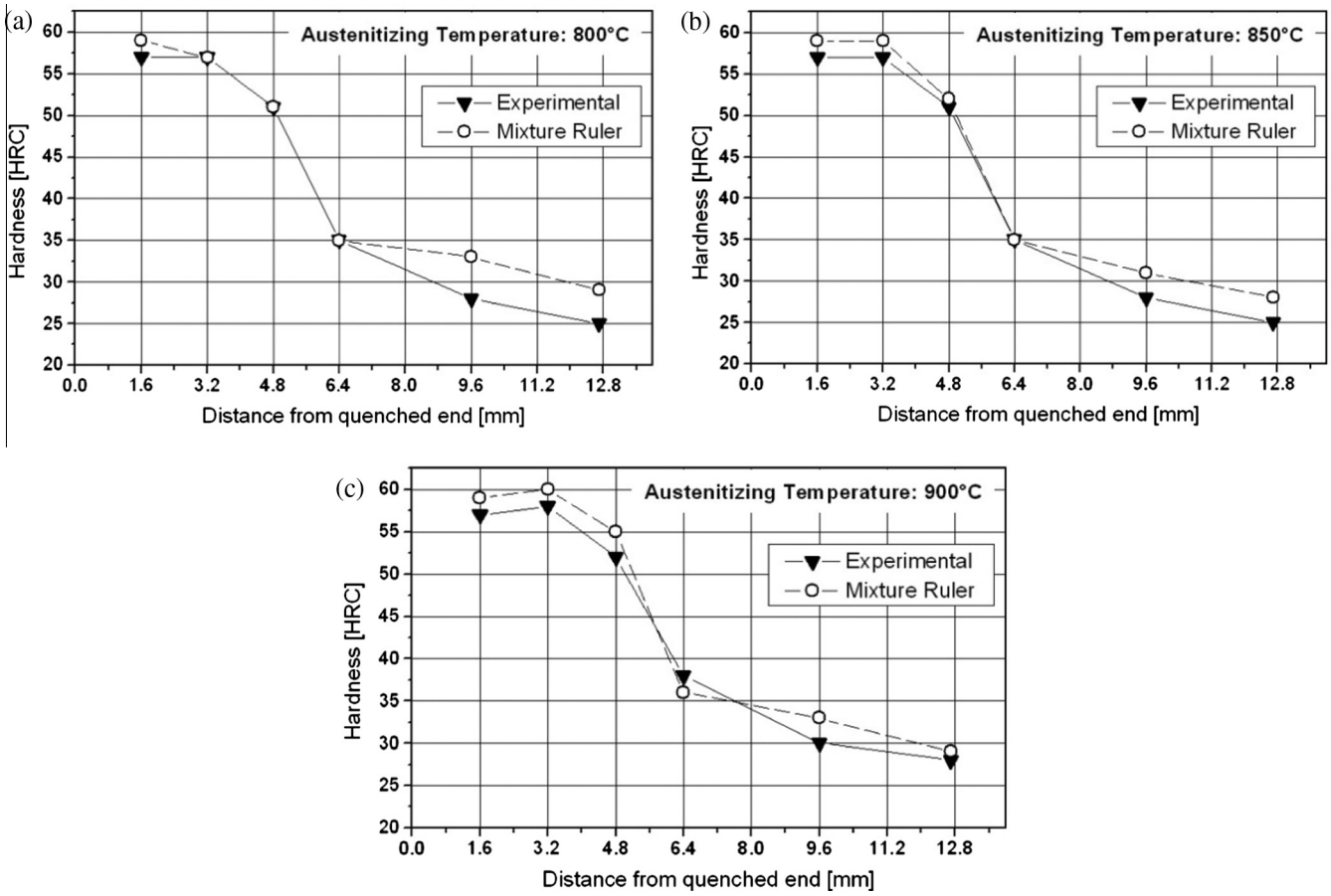

Fig. 16. Experimental hardness and calculated by mixture ruler.

martensite (light regions). In (a) and (b), formation of bainite with some probable colonies of fine pearlite and martensite can be observed. In (c), bainite formation increases with increasing of the austenitizing temperature.

Fig. 11 shows the formation of ferrite (white regions) and pearlite (dark areas). As the austenitizing temperature increases, the free ferrite formation adopts morphology acicular or needle-shaped (Fig. 11c) that penetrates into the pearlite colonies. According to [17] this acicular ferrite texture is generally associated with an increase in grain size (probably due to increasing in austenitizing temperature).

Fig. 12 shows the microstructures by Scanning Electronic Microscopy (SEM) for austenitizing temperature of 850 °C. In (a): martensite (distance from quenched end: 1.6 mm). In (b): bainite as dark areas in the form of needles (distance from quenched end: 4.8 mm). In (c): ferrite as dark areas and cementite as clear regions (distance from quench end: 12.7 mm).

According to Çakir et al. [10], Lee et al. [4] and Yao et al. [18] the microstructure altered during the Jominy test is: martensite, bainite, pearlite and ferrite in different proportions. Fernandino et al. [16] shows that for a Jominy test applied to nodular cast iron, a combination of martensite, ferrite and graphite nodules is obtained. This microstructural formation varies according to position in the specimen and to cooling rate.

3.5. Phases and micro-constituents

Tables 4–6 show the amount of phases and micro-constituents which were formed according to cooling rates during the test for each austenitizing temperature. Fig. 13 shows that while the amount of martensite and bainite reduces the amount of pearlite and ferrite increases. In both three austenitizing temperatures, the presence of bainite is evident in positions TP2 – 3.2 mm and TP3 – 4.8 mm.

However, numerical simulation results obtained by Pietrzyk and Kuziak [5] show that for a SAE 1045 steel it is possible to obtain during the test above 80% bainite. Lee et al. [4] obtained for the steel SAE 1045, using finite elements, a profile 100% bainite for a cooling distance of 10 mm. Other results according to Maizza and Matteis [11] concluded that the microstructure obtained for a SAE 4340 is: 60% martensite and 40% bainite. According to Yao [18], it is possible to obtain 100% of bainite in a steel SAE P20 Jominy test altered for the specimen with a length of 200 mm. Probably the differences in the microstructural quantities, mainly in formation of bainite, are due to the development of a numerical model for results obtained by numerical simulation, but they are not experimental data. Other variations may occur due to the chemical composition of the materials which modify the CCT curves.

3.6. Micro-hardness test

Fig. 14 shows a micro-hardness applied in a structure bainitic formed at the specimen Jominy. Fig. 15 shows micro-hardness values for each austenitizing temperature.

3.7. Hardness HRC based on the micro-hardness and percentage of phases and microconstituintes

Using the mixture ruler (Eq. (4)) and applying the results of the micro-hardness and percentages of phases, calculated hardness values were compared with those obtained experimentally, and

Fig. 16 shows this comparison. The results of the mixture ruler are presented in Rockwell C scale. In this regard Smoljan [19] used the mixing and additive rules to predict the microstructural hardness, in the same way of Zehtab et al. [7]. The mixing rules are efficient to calculate the overall hardness of the resulting microstructure in the Jominy test.

3.8. Correlation between hardness and cooling rates

Expressions that calculate hardness HV using the cooling rate and chemical composition were developed by Li [15]. In these expressions the value of the cooling rate to 700 °C is used. In this paper, we present expressions that are valid from the austenitizing temperature to room temperature. Correlation between hardness and cooling rate could be established from the data in Tables 2 and 3 permitting to obtain numerical expressions (8) for estimating hardness in function of cooling rates, austenitizing temperatures and positions according to Fig. 17.

For austenitizing temperature: 800 °C

$$\mathrm{HRC} = -64.5 \cdot \exp\left[\frac{-\overset{o}{T}}{15.2}\right] + 57.5 \tag{8}$$

For austenitizing temperature: 850 °C

$$\mathrm{HRC} = -51.6 \cdot \exp\left[\frac{-\overset{o}{T}}{23.2}\right] + 58.4 \tag{9}$$

For austenitizing temperature: 900 °C

$$\mathrm{HRC} = -58.2 \cdot \exp\left[\frac{-\overset{o}{T}}{15.5}\right] + 57.6 \tag{10}$$

3.9. Correlation between percentage of phases and cooling rates

With the percentage of the micro-constituents and phases in the microstructure of the specimen and the cooling rates, it was

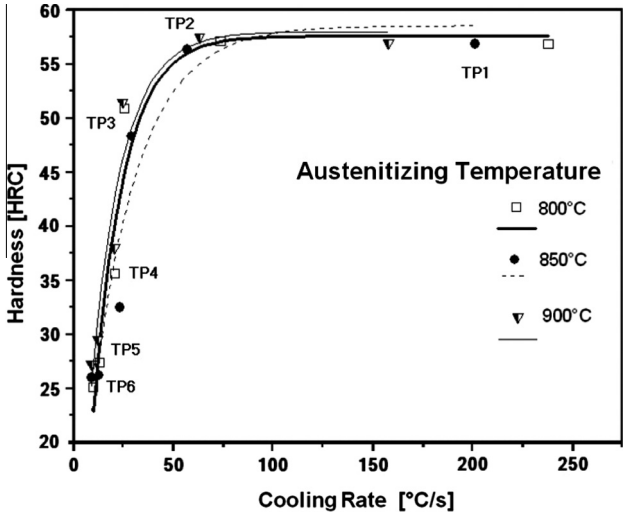

Fig. 17. Correlation between hardness and cooling rates in function of positions.

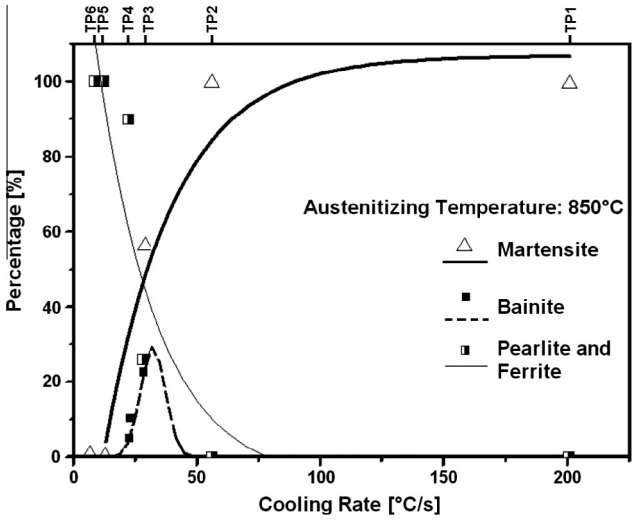

Fig. 19. Percentage of phases as a function of cooling rate for an austenitizing temperature of 850 °C.

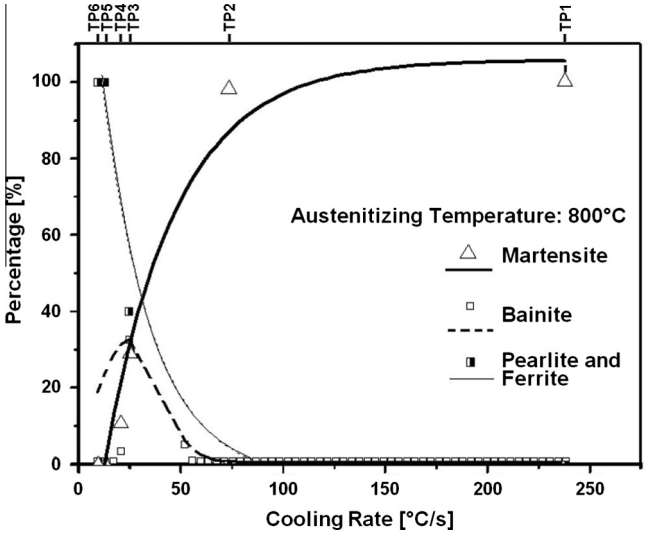

Fig. 18. Percentage of phases as a function of cooling rate for an austenitizing temperature of 800 °C.

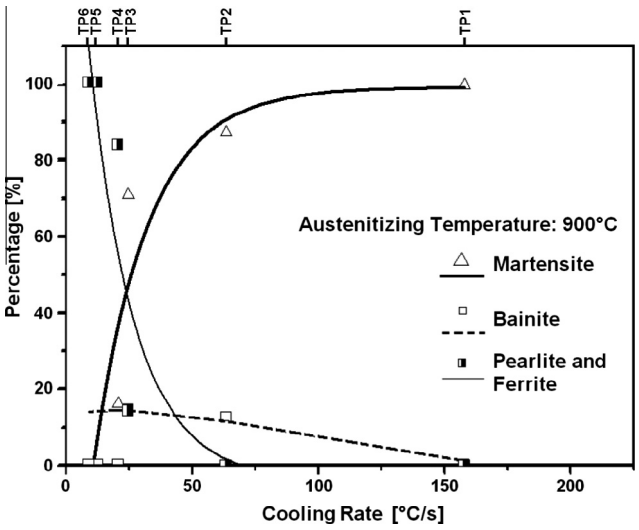

Fig. 20. Percentage of phases as a function of cooling rate for an austenitizing temperature of 900 °C.

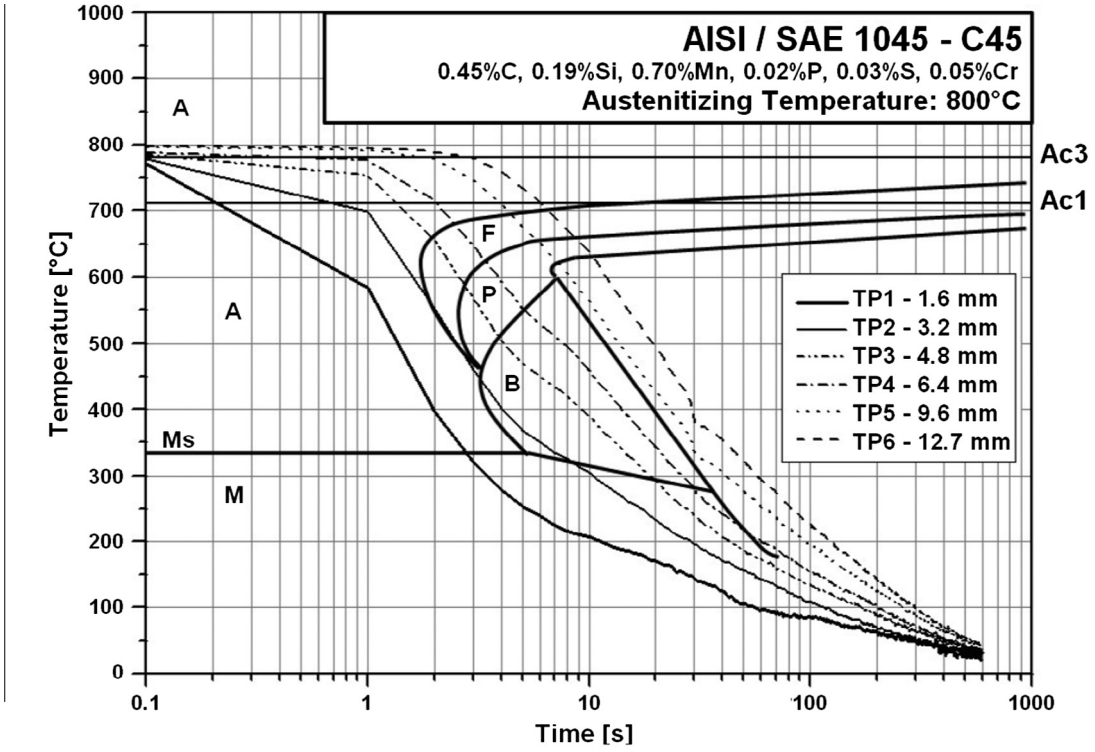

Fig. 21. Experimental cooling curves and microstructure formed during the test Jominy for SAE 1045 steel. Austenitizing temperature: 800 °C.

possible to obtain numerical expressions 11–19, which describe the presence of a particular phase in the microstructure as the cooling rate varies, as shown in Figs. 18–20.

For austenitizing temperature: 800 °C

$$\%\text{Martensite} = -149.6 \cdot \exp\left[\frac{-\overset{o}{T}}{35.2}\right] + 105.7 \tag{11}$$

$$\%\text{Bainite} = 0.51 + 32.2 \cdot \exp\left[\frac{-(\overset{o}{T} - 24.9)^2}{432.2}\right] \tag{12}$$

$$\%\text{Ferrite} + \text{Pearlite} = 168.4 \cdot \exp\left[\frac{-\overset{o}{T}}{24.8}\right] - 4.1 \tag{13}$$

For austenitizing temperature: 850 °C

$$\%\text{Martensite} = -160.9 \cdot \exp\left[\frac{-\overset{o}{T}}{28.3}\right] + 106.9 \tag{14}$$

$$\%\text{Bainite} = 3.8 \cdot \exp\left[-2\left(\frac{\overset{o}{T} - 32.1}{10.1}\right)^2\right] \tag{15}$$

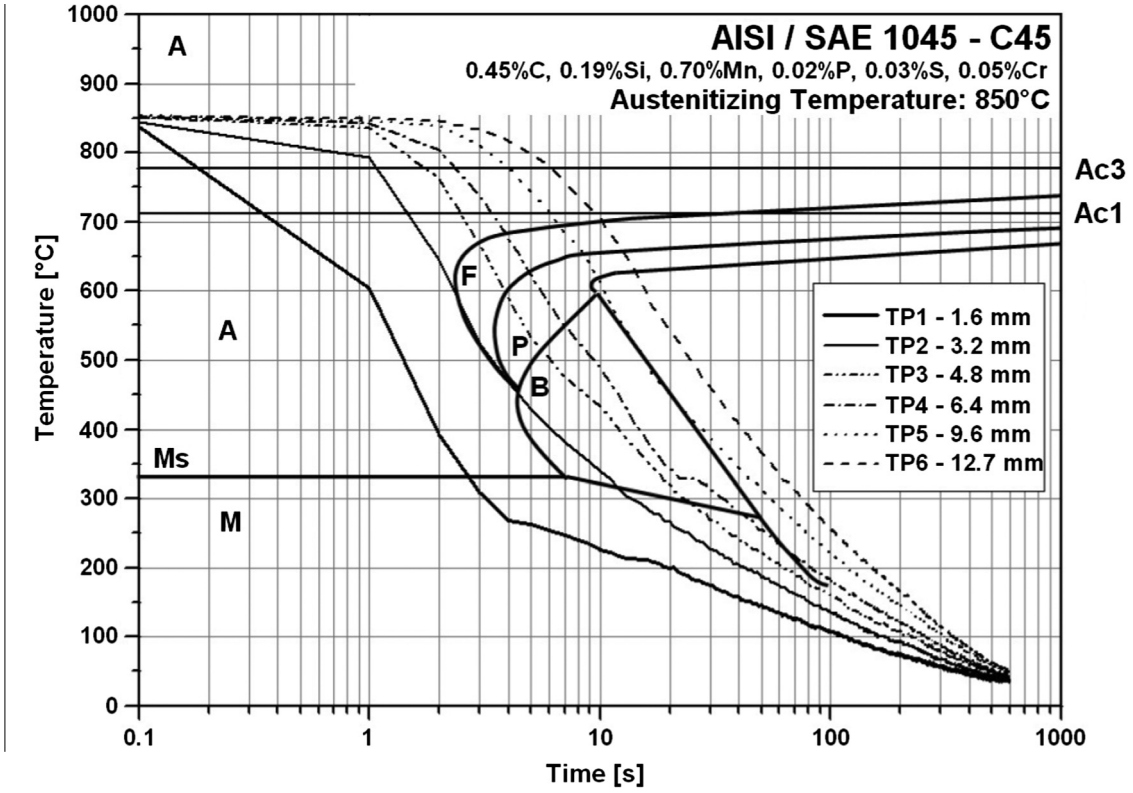

Fig. 22. Experimental cooling curves and microstructure formed during the test Jominy for SAE 1045 steel. Austenitizing temperature: 850 °C.

$$\%\text{Ferrite} + \text{Pearlite} = 168.4 \cdot \exp\left[\frac{-\overset{o}{T}}{24.6}\right] - 6.6 \tag{16}$$

For austenitizing temperature: 900 °C

$$\%\text{Martensite} = -161.9 \cdot \exp\left[\frac{-\overset{o}{T}}{21.5}\right] + 99.4 \tag{17}$$

$$\%\text{Bainite} = 14.4 \cdot \exp\left[-\left(\frac{\overset{o}{T} - 24.5}{432.2}\right)^2\right] \tag{18}$$

$$\%\text{Ferrite} + \text{Pearlite} = 186.9 \cdot \exp\left[\frac{-\overset{o}{T}}{17.9}\right] - 3.7 \tag{19}$$

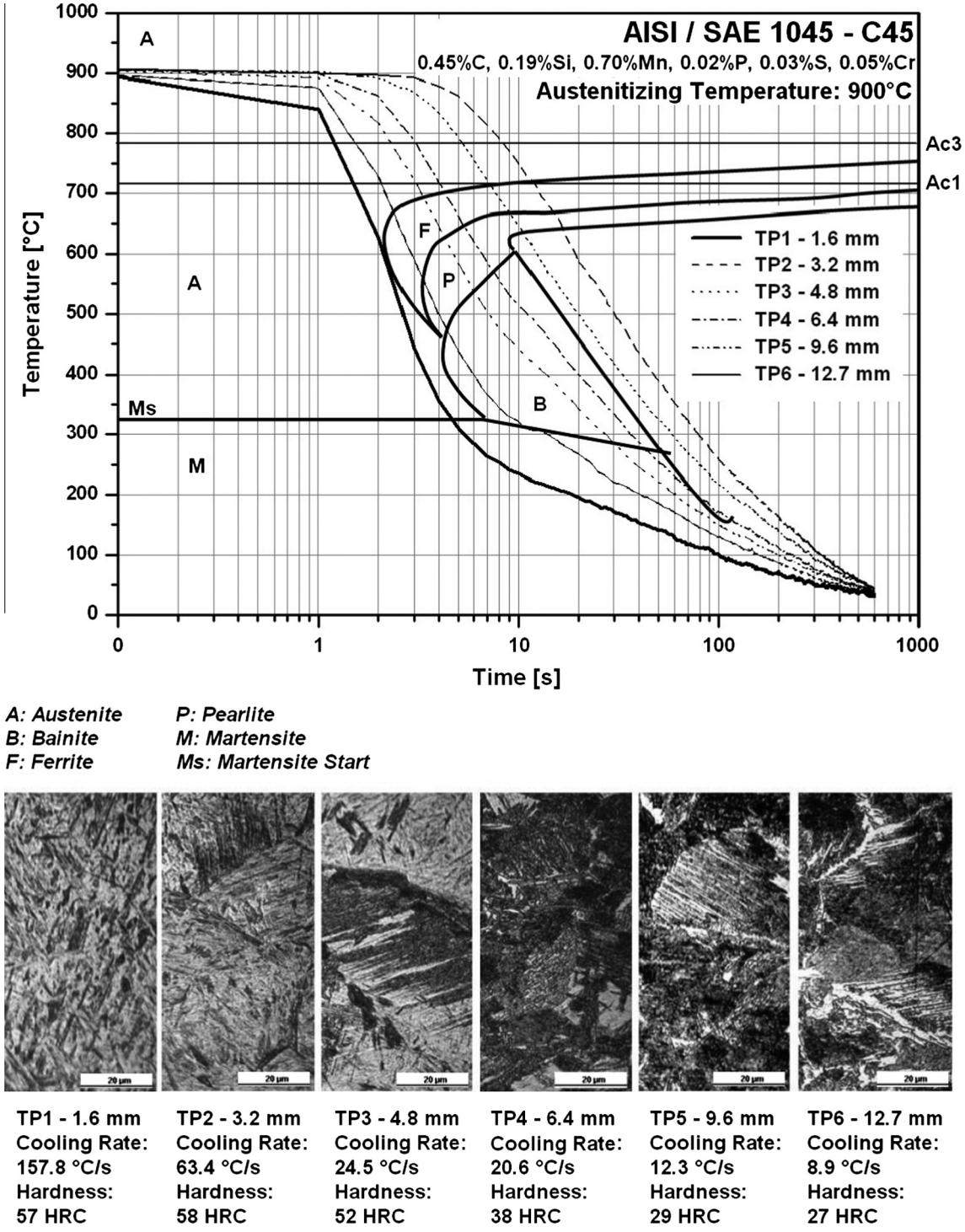

Fig. 23. Experimental cooling curves and microstructure formed during the test Jominy for SAE 1045 steel. Austenitizing temperature: 900 °C.

3.10. Correlation between experimental cooling curves and Continuous Cooling Transformation diagrams – CCT

The cooling curves obtained experimentally for the Jominy test were confronted with CCT diagrams in order to predict the possible formed microstructures during the test. Figs. 21–23 show the cooling curves superimposed on a CCT diagram for AISI 1045 steel [20]. For the three austenitizing temperatures, it was observed that is possible during the continuous cooling to obtain different structures. At position TP1 when the temperature decreases as a function of time the thermal curve crosses only the region of martensite formation. At position TP2 it is formed a certain amount of bainite and martensite. In the TP3 and TP4 positions, there is the formation of ferrite, pearlite, bainite, and the martensite is formed in smaller amounts, as explained in Fig. 13. Finally, at the TP5 and TP6 positions, with lower cooling rates, only occurs the

formation of ferrite and pearlite for this type of steel. Çakir et al. [10] and Trzaska et al. [21] demonstrated that the use of thermocouples for the cooling curves is efficient. The CCT curves are an excellent graphical tool to compare the curves with the microstructure resulting from experimental or simulated trial, according to [20].

4. Conclusions

The following major conclusions can be drawn from the present study:

(1) It was observed that the morphology of the obtained phases was altered according to the austenitizing temperature.
(2) For the high austenitizing temperature, it was observed an increase in Jominy hardness profile.
(3) The calculated hardness values based on mixture ruler are in good agreement with the experimental results.
(4) Based on the good agreement between experimental and theoretical calculated hardness, expression for the percentage of phases in function of cooling rates could be determined.
(5) Numerical expressions have been developed describing microstructure formation as the cooling rates varies during the Jominy test. These expressions provide an insight into the determining of austenitizing temperature in terms of structures and hardness.

Acknowledgements

The authors would like to acknowledge support provided by Coordination for the Improvement of Higher Level or Education (CAPES), The Pontifical Catholic University of Rio Grande do Sul – Brazil (PUCRS), The Institute of Applied Engineering TECSUP (Perú) and The Federal University of Rio Grande do Sul – Brazil (UFRGS), Foundry Laboratory (LAFUN): special thanks to Dr. J.A. Spim due to his outstanding accomplishments in the area of metallurgy and materials, his dedication to the research, and his profound effect on people and students in the universities. We are grateful to have had the privilege to learn from such a great man as Dr. Spim, who was and still in an inspiration.

References

[1] D. Homberg, A numerical simulation of the Jominy end-quench test, Acta Mater. 44 (1996) 4375–4385.
[2] P. Le Masson, T. Loulou, P. Rogeon, D. Carron, J. Quemener, A numerical study for the estimation of a convection heat transfer coefficient during a metallurgical "Jominy end-quench" test, Int. J. Therm. Sci. 41 (2002) 517–527.
[3] B. Smoljan, Mathematical modeling of austenite decomposition during the quenching, in: 13th International Scientific Conference on Achievements in Mechanical and Materials Engineering, Gliwice – Wisla, Poland, 2005.
[4] S. Lee, E. Pavlina, C.H. Van Tyne, Kinetics modeling of austenite decomposition for an end-quenched 1045 steel, Mater. Sci. Eng., A 527 (2010) 3186–3194.
[5] M. Pietrzyk, R. Kuziak, Computer aided interpretation of results of the Jominy test, Arch. Civil Mech. Eng. 11 (2011) 707–722.
[6] B. Smoljan, D. Iljkic, H. Smokvina, F. Traven, An analysis of modified Jominy test, Comput. Mater. Sci. Surf. Eng. 1 (2009) 120–124.
[7] A. Zehtab, S. Sajjadi, S. Zebarjad, S. Nezhad, Prediction of hardness at different points of Jominy specimen using quench factor analysis method, J. Mater. Process. Technol. 99 (2008) 124–129.
[8] Y. Song, G. Liu, S. Liu, J. Liu, C.H. Feng, Improved nonlinear equation method for numerical prediction of Jominy end-quench curves, J. Iron. Steel Res. Int. 14 (2007) 37–41.
[9] T. Ghrib, F. Bejaoui, A. Hamdi, N. Yacoubi, Correlation between thermal properties and hardness of end-quench bars for C48, 42CrMo4 and 35NiCrMo16 steels, Thermochim. Acta 473 (2008) 86–91.
[10] M. Çakir, A. Ozsoy, Investigation of the correlation between thermal properties and hardenability of Jominy bars quenched with air–water mixture for AISI 1050 steel, Mater. Des. 32 (2011) 3099–3105.
[11] G. Maizza, P. Matteis, Modeling of Jominy end-quench test of multiphase steels by means of Comsol script, in: Excerpt from Proceedings of the COMSOL Users Conference, Grenoble, 2007.
[12] ASM Handbook Committee, Heat Treatment, ASM International, V4, 1985, p. 104.
[13] P. Li, B. Xiong, Y. Zhang, Z. Li, B. Zhu, F. Wang, H. Liu, Quench sensitivity and microstructure character of high strength AA7050, Trans. Nonferr. Met. Soc. China 22 (2012) 268–274.
[14] Y. Ben Ammar, A.M. Aoufi, Darrieulat, Influence of the cooling rate on the texture and the microstructure of Zircaloy-4 studied by means of a Jominy end-quench test, Mater. Sci. Eng., A 556 (2012) 184–193.
[15] M. Li, D. Niebuhr, L. Meekisho, D. Atteridge, A computational model for the prediction of steel hardenability, Metall. Mater. Trans. B 29B (1998) 661–672.
[16] D. Fernandino, J. Massone, R. Boeri, Characterization of the austemperability of partially austenitized ductile iron, J. Mater. Process. Technol. 213 (2013) 1801–1809.
[17] D. Llewellyn, R. Hudd, Steels. Metallurgy and Applications, third ed., Butterworth-Heinemann, Oxford, United Kingdom, 2004, p. 210.
[18] X. Yao, J. Gu, M. Hu, Z. Zhu, A numerical study of an insulating end-quench test for high hardenability steels, Scand. J. Metall. (2003).
[19] B. Smoljan, S. Smokvina, N. Tomasic, D. Iljkic, Computer simulation of microstructure transformation in heat treatment processes, J. Achiev. Mater. Manuf. Eng. 24 (2007) 275–282.
[20] G.F. Vander Voort, Atlas of Time-Temperature Diagrams for Irons and Steels, ASM International, PA, United States, 2007.
[21] J. Trzaska, A. Jagiello, L. Dobrzanski, The calculation of CCT diagrams for engineering steels, Arch. Mater. Sci. Eng. 39 (2009) 13–20.